Received: 11 May 2023 | Revised: 26 July 2023 | Accepted: 2 August 2023

DOI: 10.1111/ejss.13405

RESEARCH ARTICLE

European Journal of Soil Science WILEY

Small lateral air pressure gradients generated by a large chamber system have a strong effect on CO_2 transport in soil

Laurin Osterholt[1,2] | Martin Maier[1] | Dirk Schindler[3]

[1]Department of Crop Science, Division Soil Physics, University of Göttingen, Göttingen, Germany

[2]Department of Soil and Environment, Forest Research Institute Baden-Württemberg, Freiburg, Germany

[3]Environmental Meteorology, Albert-Ludwigs-University of Freiburg, Freiburg, Germany

Correspondence

Laurin Osterholt, Division Soil Physics, University of Göttingen, Department of Crop Science, Grisebachstraße 6, Göttingen 37077, Germany.

Email: laurin.osterholt@uni-goettingen.de

Funding information

Deutsche Forschungsgemeinschaft, Grant/Award Number: MA 5826/2-2

Abstract

Gas transport in soils is usually assumed to be purely diffusive, although several studies have shown that non-diffusive processes can significantly enhance soil gas transport. These processes include barometric air pressure changes, wind-induced pressure pumping and static air pressure fields generated by wind interacting with obstacles. The associated pressure gradients in the soil can cause advective gas fluxes that are much larger than diffusive fluxes. However, the contributions of the respective transport processes are difficult to separate. We developed a large chamber system to simulate pressure fields and investigate their influence on soil gas transport. The chamber consists of four subspaces in which pressure is regulated by fans that blow air in or out of the chamber. With this setup, we conducted experiments with oscillating and static pressure fields. CO_2 concentrations were measured along two soil profiles beneath the chamber. We found a significant relationship between static lateral pressure gradients and the change in the CO_2 profiles ($R^2 = 0.53$; p-value <2e-16). Even small pressure gradients between −1 and 1 Pa relative to ambient pressure resulted in an increase or decrease in CO_2 concentrations of 8% on average in the upper soil, indicating advective flow of air in the pore space. Positive pressure gradients resulted in decreasing, negative pressure gradients in increasing CO_2 concentrations. The concentration changes were probably caused by an advective flow field in the soil beneath the chamber generated by the pressure gradients. No effect of oscillating pressure fields was observed in this study. The results indicate that static lateral pressure gradients have a substantial impact on soil gas transport and therefore are an important driver of gas exchange between soil and atmosphere. Lateral pressure gradients in a comparable range can be induced under windy conditions when wind interacts with terrain features. They can also be caused by chambers used for flux measurements at high wind speed or by fans used for head-space mixing within the chambers, which yields biased flux estimates.

KEYWORDS
advective flux, chamber flux measurements, static air pressure fields, wind-induced pressure pumping

1 | INTRODUCTION

Soils are an important source or sink of different greenhouse gases and play an important role in the global carbon budget (Schlesinger & Andrews, 2000). For estimating ecosystem carbon (C) and nitrogen (N) budgets, gaseous fluxes of C and N from soils are highly relevant, and they contain important greenhouse gases such as CO_2, CH_4 and N_2O. The production of a gas species in soil and the instantaneous flux between soil and atmosphere are not the same (Elberling, 2003; Maier et al., 2011) since the gases produced in the soil need to travel from the location of production to the atmosphere and because of biological or chemical processes (such as methane oxidation) consuming or altering the gas in soil. Therefore, soil gas transport rates are an essential factor. Various climatic drivers and soil parameters influence soil gas transport. While soil parameters such as total porosity and soil structure only underlie spatial variability but remain relatively constant on a temporal scale except for special conditions, like freezing and thawing or shrinkage of cracks in clayey soils, changes in climatic drivers lead to changing conditions of soil gas transport over time. The main climatic drivers are (1) precipitation and evaporation, which control soil moisture and hence the air-filled pore space, and (2) soil temperature, which is the main driver for biological activity in soil controlling the production or consumption of gases in soil (Smith et al., 2003).

Soil gas transport is usually dominated by diffusion, but if pressure gradients are present in the soil also non-diffusive transport processes such as advective gas flow can occur. Even if pressure gradients are relatively small, the resulting advective fluxes can be much larger than diffusive fluxes (Scanlon et al., 2002). Pressure gradients in the soil can result from different phenomena. Changes in barometric pressure can create transient pressure gradients between soil and atmosphere that result in enhanced gas transport (Clements & Wilkening, 1974; Levintal et al., 2020). Steady wind interacting with terrain features can cause static pressure fields that have been shown to create advective fluxes in porous media (Amos et al., 2009; Bowling & Massman, 2011). Rajewski et al. (2014) investigated the impact of pressure fields created by wind farms on surface fluxes and found enhanced CO_2 fluxes in the lee of the turbines. Bahlmann et al. (2020) observed that increasing near-surface wind velocity accelerates soil-atmosphere gas exchange. Other

Highlights

- We developed a chamber system to simulate static and oscillating pressure fields.
- Oscillating pressure fields had no discernible effect on soil gas transport.
- Static pressure fields had a substantial effect on soil gas transport.

studies have found that wind-induced pressure pumping can increase transport rates in soil (Laemmel, Mohr, Longdoz, et al., 2019; Takle et al., 2004). Pressure pumping describes pressure fluctuations generated by above-canopy wind turbulence that propagate into the soil. The term pressure pumping is not consistently used in literature; in this study, it refers to pressure oscillations with a frequency of around 0.01 Hz, according to Mohr et al. (2016). These pressure fluctuations do not lead to net advective flux when integrating over a time period covering multiple high- and low-pressure periods, but through the oscillation of the air column in the soil pore system an increase in transport rates can be observed due to dispersion (Laemmel, Mohr, Longdoz, et al., 2019).

Gas fluxes between soil and atmosphere are commonly estimated by chamber measurements (Maier et al., 2022). This technique assumes diffusive gas transport, which is not always given, especially under conditions when pressure gradients might occur. Additionally, the chamber itself can induce a pressure gradient between chamber and ambient atmosphere, for example, under windy conditions due to the Venturi effect when using an inappropriate vent design (Xu et al., 2006). Such pressure gradients can strongly bias the resulting flux estimate. Therefore, the understanding of non-diffusive transport processes is important to identify situations under which chamber flux measurements might not be reliable or to develop methods that enable robust flux estimates under such conditions.

The non-diffusive transport processes need to be better understood. On the one hand, the in situ monitoring of gas transport is technically challenging and interactions between different environmental drivers (e.g., wind often coincides with rain) make it hard to interpret the results on a process level. On the other hand, laboratory measurements with soil cores disregard macro-structures and effects due to changing environmental drivers are not involved. Additionally, naturally occurring oscillating or static pressure fields are not one- but two-dimensional air pressure fields at the ground surface that result in both vertical and lateral pressure gradients in the soil (Clarke & Waddington, 1991). This three-dimensional component of pressure fields is difficult to represent in laboratory experiments (Laemmel, Mohr, Schack-Kirchner, et al., 2019). Yet, a better understanding of non-diffusive transport processes is important to improve ecosystem flux estimates under windy conditions. Therefore, this study aims to develop a chamber system to simulate (a) oscillating and (b) static pressure fields and to investigate their effect on soil gas transport.

2 | METHODS

2.1 | Chamber design

We developed a large chamber system (Figure 1) to artificially generate oscillating and static pressure fields. This enables us to investigate their quantitative effect on soil gas exchange for a specific soil under controlled conditions.

The chamber is constructed with a framework of poles covered by a plastic tarp. The base area of the chamber is 2 × 3.2 m and the chamber height is 0.8 m. The chamber is divided into four subspaces (width = 0.8 m) that can be used to generate lateral pressure gradients. To obtain a pressure-tight connection to the soil, the chamber is placed on a base made of sheet metal that is driven into the ground to a depth of about 0.02 m.

Fans that continuously blow air in and out of the chamber on both sides of each subspace ensure continuous gas exchange with the atmosphere. This prevents an accumulation of CO_2 inside the chamber. At the bottom, homogeneous air circulation is achieved by fans installed directly above the soil. The slow air circulation at the bottom is separated from the circulation in the upper part by an air-permeable fabric spanned at about 0.4 m. This feature enables us to differentiate between the effect of pressure fields generated at the top of the chamber system and the influence of wind speed directly above the soil as simulated by the fan in the bottom part of the chamber system. To reduce the bias created by pressure fields generated by the fans, we used fans with low rotation velocities that are not directly directed towards the soil surface. In a prior experiment (shown in Appendix S1, S2) we ran the fans in the bottom part of the chamber system at different fan speeds to test the influence on the CO_2 profiles and to prevent a bias of this effect in further experiments. At high fan speeds (fans running on 60% of their capabilities or more) we observed a reaction of the CO_2 profiles. When the fans were running at 30% or lower, no influence on the CO_2 profiles was observed. During further experiments, we ran the fans at 0% (which is the slowest possible speed before they stop turning). To minimize air temperature changes inside the chamber due to insolation and to protect the chamber from precipitation, a second tarp was installed approximately 0.5 m above the chamber.

The pressure fields are generated by additional fans blowing air either into or out of each subspace. The resulting pressure inside the subspaces is regulated by adjusting the fan speed with a microcontroller (Arduino UNO R3) via pulse width modulation. Each subspace can be controlled individually. This enables to automatically run a program where pressure conditions inside the individual subspaces are altered stepwise over several days. Pressure pumping can be simulated by alternately blowing air in and out of the chamber. The pressure pumping coefficient (*PPC*), as defined by Mohr et al. (2016), quantifies the intensity of pressure pumping. *PPC* is the mean absolute slope of pressure against time between the subsequent measurement points in a 30-min interval.

The pressure gradient between the chamber system and the surrounding atmosphere is measured in each subspace with differential pressure sensors (SSCSNBN001NDAA5, TruStability® Board Mount Pressure Sensors, Honeywell). The sensors have a measurement range between −250 and 250 Pa, a resolution of

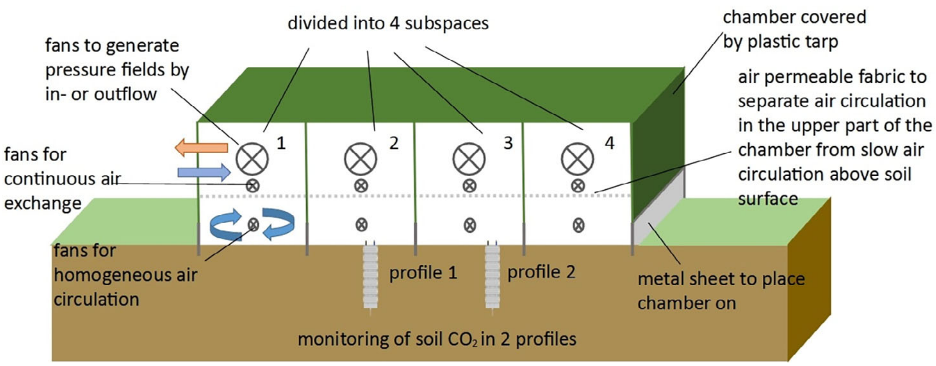

FIGURE 1 Chamber system with four subspaces, each equipped with several fans that ensure continuous air exchange and generate pressure fields by blowing air into or out of the chamber.

0.1 Pa and an accuracy of about 0.6 Pa. Natural pressure fluctuations were measured outside the chamber system with a set-up as described by Mohr et al. (2020). The natural pressure fluctuation measurements were used to differentiate between the effect of the pressure fields generated by the chamber and naturally occurring turbulence that might have an influence on pressure conditions inside the chamber.

2.2 | Monitoring set-up and data processing

The gas exchange between soil and atmosphere inside the chamber has been monitored by two CO_2 profile probes with built-in sensors, as described by Osterholt et al. (2022). The probes measure CO_2 concentrations continuously in seven depths (3.5, 7, 10.5, 14, 17.5, 21 and 24.5 cm) underneath the chamber. Profile 1 was located in subspace 2 and profile 2 was in subspace 3. The distance from the profiles to the outer border of the chamber was comparable (≈ 0.7 m), whereas profile 1 was about 0.1 m closer to the inner border between subspace 2 and 3 (0.4 m) than profile 2 (0.5 m).

For data processing and visualization, we used the programming language R (version 4.0.5, R Core Team, 2021). To identify the effect of the applied pressure fields on the CO_2 profiles, CO_2 concentrations from before and after each experiment were interpolated using a generalized additive model using the package mgcv (version 1.8.34, Wood, 2017) that was fit to the CO_2 concentrations as a function of time for each depth. The interpolated CO_2 concentration was assumed to represent the no-treatment CO_2 profile that would have been observed if no pressure field had been applied. The difference between the interpolated CO_2 concentrations and the measured CO_2 during the experiment describes the change in CO_2 (*CO_2-shift*) that is caused by the pressure field. To compare the change in CO_2 over different depths and between experiments with different absolute CO_2 values, *CO_2-shift* is described as the percentage of the absolute CO_2 concentration.

Beneath subspace 1, five soil moisture sensors (ECH_2O EC-5 Soil Moisture Sensor, Decagon Devices) were installed in the following depths: two sensors in 7 cm, two sensors in 14 cm and one sensor in 21 cm. Air temperature was measured directly above the soil inside the chamber in subspace 2.

2.3 | Study site and experimental design

The setup was first tested in a sandpit outside the laboratory and then installed in a Scots pine forest at the meteorological experimental site in Hartheim (Upper Rhine Valley, southwest Germany), where the effect of wind-induced pressure pumping has been investigated and quantified in earlier studies (Laemmel, Mohr, Longdoz, et al., 2019). The soil is a Haplic Regosol (FAO, 2006) with a humus type of mull, an Ah horizon (0–0.15 m) consisting of loamy silt and a transitional Ah/C horizon (0.15–0.40 m) where the fraction of gravel and sand increases with depth. The site is equipped with permanent meteorological monitoring infrastructure such as precipitation and above canopy wind speed. These data were used to ensure that changing meteorological conditions did not interfere with the experiments. The chamber system was installed on forest floor consisting of a thin L-mull humus layer and sparse ivy (Hedera Helix, L.) vegetation.

We conducted several experiments with static pressure fields, oscillating pressure fields (pressure pumping) and a combination of the two (Table 1). The four modes of static pressure fields included lateral pressure gradients between the subspaces ($P_{lateral}$) from higher to lower pressure or vice versa and a homogeneous positive or negative pressure over all subspaces (Figure 2). For the lateral pressure gradient experiments, we treated subspaces 1 and 2 as well as subspaces 3 and 4 identically so that pressure conditions were comparable among these pairs of subspaces, only between subspaces 2 and 3 a distinct pressure gradient was applied. Static pressure fields range from −1 to 1 Pa relative to ambient pressure. For each static pressure field experiment, we applied the four modes successively each for 6–8 h without lag times between the different modes. Between the replications of the experiments, we let the concentration profiles stabilize for at least 8 h.

$P_{lateral}$ was defined as the difference between pressure in subspace 1 and 3 for profile 1. To account for the direction of the lateral pressure gradient, $P_{lateral}$ for profile 2 was defined as the inverse $P_{lateral}$ of profile 1 so that $P_{lateral}$ (profile 1) = -$P_{lateral}$ (profile 2). We used pressure values from subspaces 1 and 3 for the calculation of $P_{lateral}$ since these sensors provided the most stable signal during the whole study period, especially in subspace 2, the pressure signal showed artefacts due to ambient pressure changes as documented in Section 3.1. Pressure readings were highly correlated between subspaces 3 and 4 (r = 0.96) and also well correlated between subspaces 1 and 2 (r = 0.78) when periods with ambient *PPC* >0.1 were excluded, correlation between subspaces 1 and 2 could be increased (r = 0.84) indicating that the sensor in subspace 2 was more reliable under calm conditions without ambient pressure changes.

For the pressure pumping experiments, *PPC* was increased or decreased stepwise in a range between 0.15 and 0.6 Pa/s. Each pressure pumping experiment consists of three steps with constant *PPC* for 6 h. We used both

TABLE 1 Description of the different modes of pressure fields generated in the chamber.

Mode	Description	P range	Replications
High P	Static positive pressure in all subspaces	0.5 to 1 Pa	9
Low P	Static negative pressure in all subspaces	−0.5 to −1 Pa	9
$P_{lateral}$	Persistent pressure gradient between the subspaces (positive in subspaces 1 and 2 (1 Pa) and negative in 3 and 4 (−1 Pa) or vice versa)	−1 to 1 Pa	9
PP	Oscillating pressure in all subspaces (pressure pumping) (period: 60 s; $\lvert P_{lateral}\rvert < 0.1$ Pa)	−10 to 10 Pa	9
PP & $P_{lateral}$	Oscillating pressure and static lateral pressure gradient (period: 60 s; $\lvert P_{lateral}\rvert > 0.1$ Pa)	−10 to 10 Pa	11

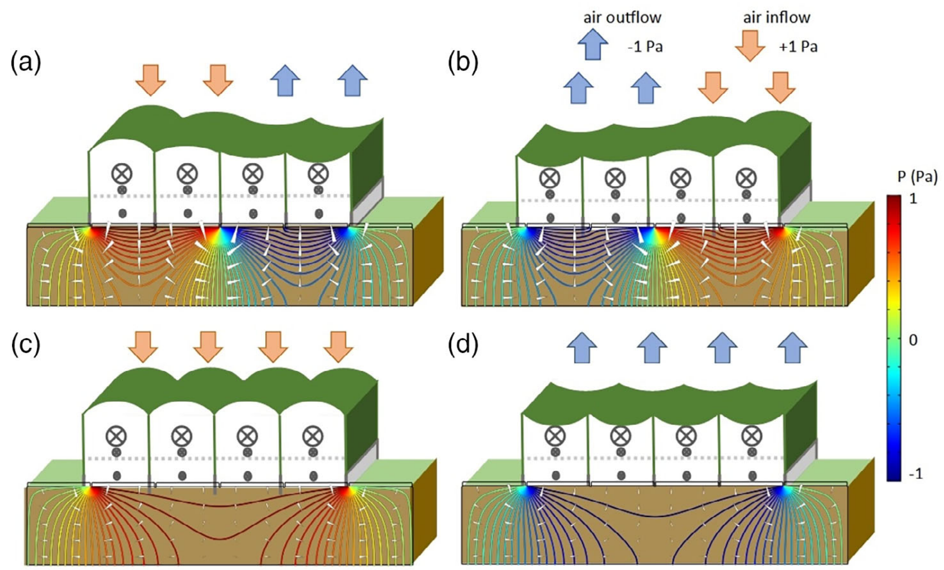

FIGURE 2 The different scenarios of pressure fields: (a) Lateral pressure gradient between the subspaces from higher pressure on the left to lower pressure on the right and (b) vice versa. Homogeneous pressure fields with (c) higher pressure or (d) lower pressure in the chamber relative to ambient pressure. The lateral pressure gradients generate advective gas flow between the subspaces, which is visualized by the white arrows that illustrate the direction and magnitude of the flux. For the visualization of pressure gradients in soil, we set up a simplified 2D model using the finite element modelling software COMSOL (Comsol Multiphysics 5.2a, Burlington, USA).

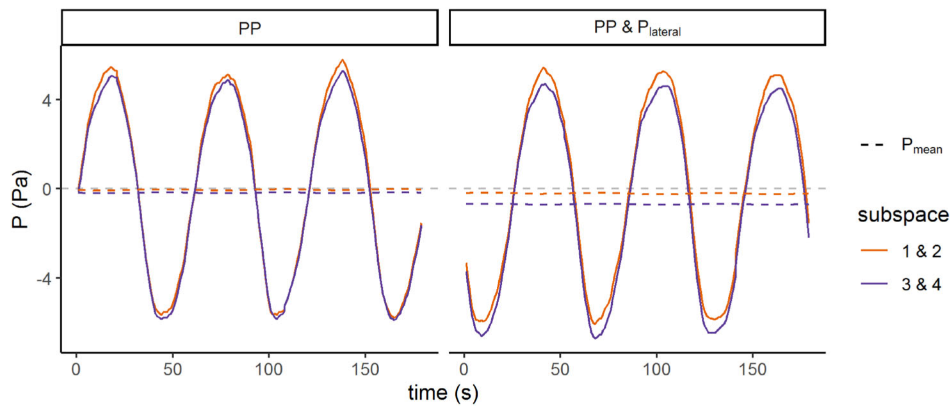

FIGURE 3 Pressure oscillation in the subspaces of the chamber system during the pressure pumping experiments. In the left panel, P_{mean} is close to zero in all subspaces. In the right panel, P_{mean} differs from zero and a lateral pressure gradient between the subspaces is present. For clarity, subspaces 1 & 2 and 3 & 4 were combined.

decreasing and increasing *PPC* steps to avoid a systematical bias due to an influence of the previous *PPC* step since the concentration profiles need several hours to reach steady state after conditions have changed. Natural pressure pumping does not lead to a net advective flux between soil and atmosphere since the average pressure gradient is zero when averaged over several minutes. However, in our chamber system, small differences

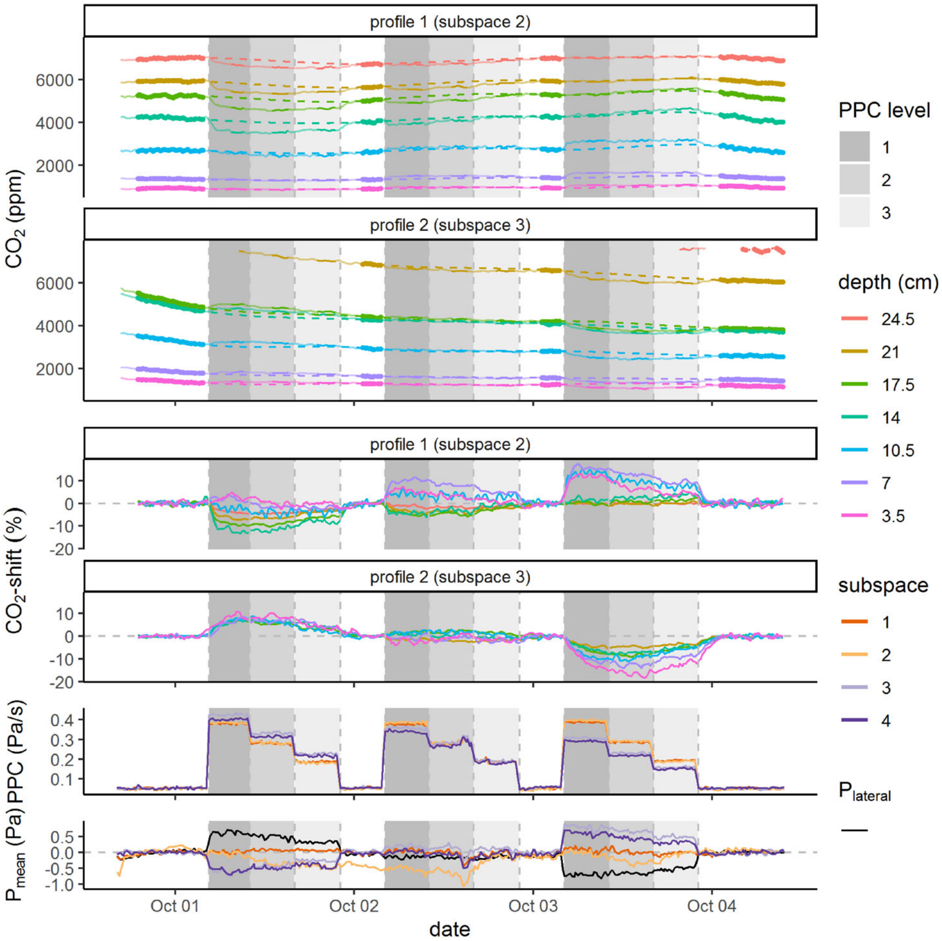

FIGURE 4 Experiments with pressure pumping and changing $P_{lateral}$. Each experiment has three levels of pressure pumping intensity. The first experiment with P_{mean} around 0.5 Pa in subspaces 3 and 4, the second experiment with $P_{lateral}$ close to zero and the third experiment with P_{mean} around −0.5 Pa in subspaces 3 and 4.

between inflow and outflow rates can lead to pressure gradients between the inside of the chamber and the ambient atmosphere that turned out to be different from zero on average. This net pressure gradient was identified by applying a moving average on the pressure signal (P_{mean}) with a window size of 20 min, which covers several pressure pumping periods (60 s). To regulate P_{mean} during the pressure pumping experiments, the pressure-generating fans were regulated to different speeds during the inflow and outflow periods. Figure 3 shows a short time period of the simulated pressure oscillations with and without $P_{lateral}$.

3 | RESULTS

The influences by environmental conditions such as soil moisture and air temperature could be successfully excluded by converting the absolute CO_2 concentrations to the relative unit *CO_2-shift* when comparing the effect between the different experiments. While the absolute CO_2 concentration showed a clear dependency on air temperature (R^2 between 0.6 and 0.9 for the different depths) with the strongest temperature effect in the deeper depths, no discernible dependency of *CO_2-shift* on air temperature was observed ($R^2 < 0.1$ in the selected depths, mostly below 0.01). In cold periods with temperatures below 10°C also soil moisture had a strong effect on absolute CO_2 concentrations (R^2 between 0.2 and 0.8 in the selected depths), while for the warm periods, the temperature effect was dominating. By converting the concentrations to *CO_2-shift* also the soil moisture dependency could be excluded ($R^2 < 0.1$ in the selected depths, mostly below 0.01).

During storm events, a weak but discernible influence of natural pressure pumping on the pressure conditions inside the chamber system could be observed. To exclude a potential influence of this natural turbulence during the experiments, measurements with natural *PPC* above 0.15 Pa/s were excluded from the time series for further data analysis.

3.1 | Pressure pumping

The experiments with oscillating pressure fields had no detectable effect on the gas profiles. Figure 4 shows three exemplary experiments with artificial pressure pumping and changing $P_{lateral}$. In each experiment, three levels of

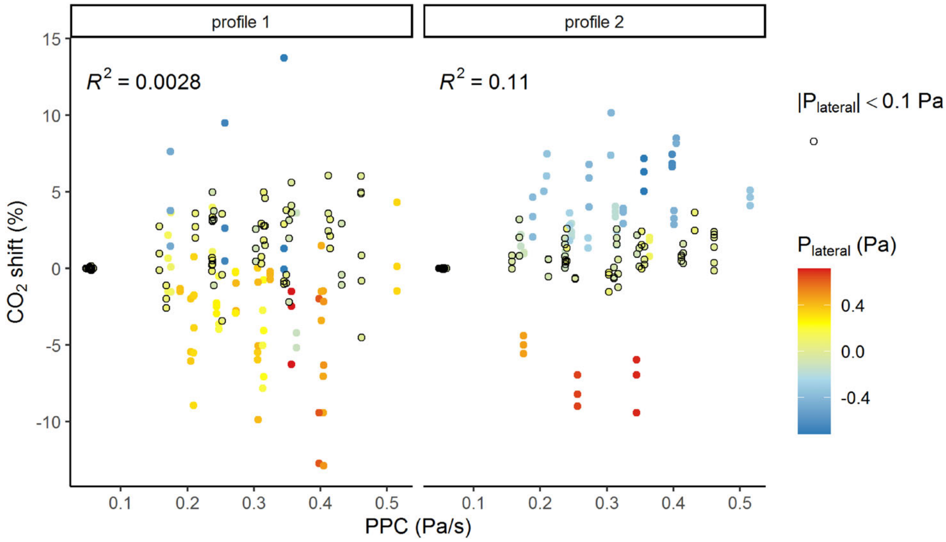

FIGURE 5 Relationship between *PPC* and *CO_2-shift*. Data from 20 experiments are combined (*PP* and *PP* & $P_{lateral}$). The colour scale illustrates the influence of $P_{lateral}$. The black circles mark the experiments with no apparent lateral pressure gradient ($P_{lateral}$ between −0.1 and 0.1 Pa).

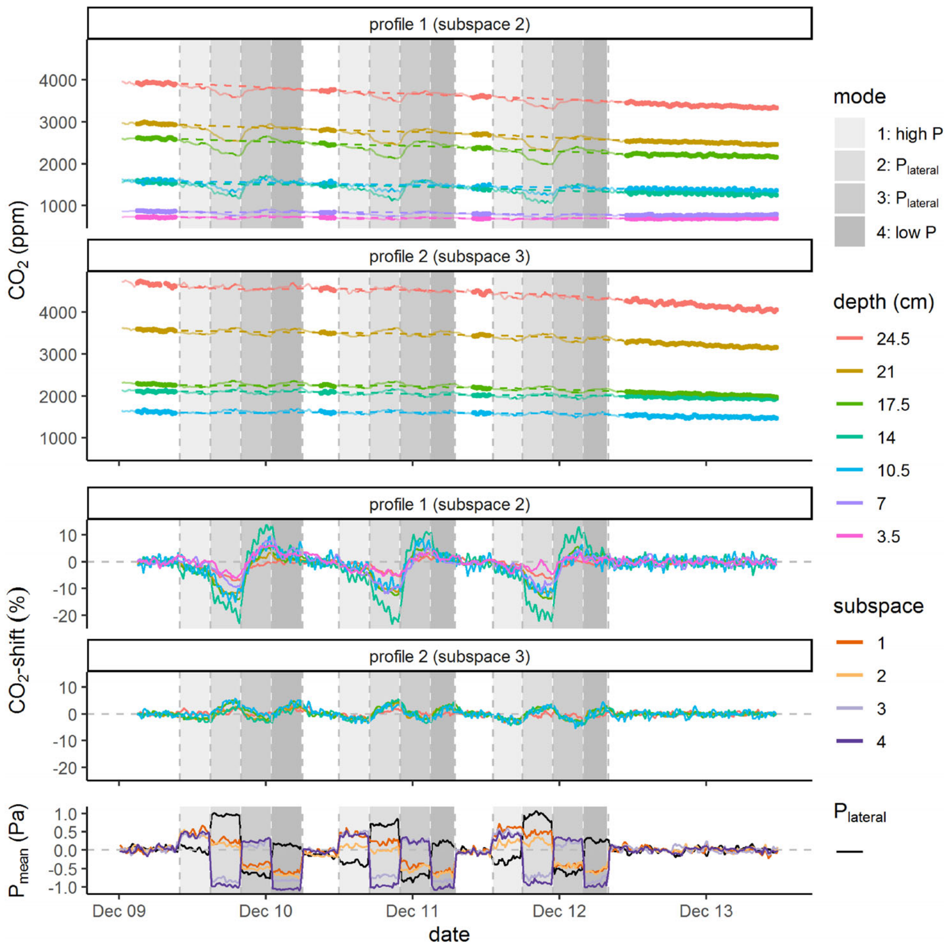

FIGURE 6 Three experiments each with four modes of static pressure fields. Mode 1: static positive pressure; Mode 2: lateral pressure gradient with negative pressure in subspaces 3 and 4; Mode 3: lateral pressure gradient with negative pressure in subspaces 1 and 2; Mode 4: static negative pressure.

PPC were applied. The first experiment with negative P_{mean} in subspaces 3 and 4, the second experiment with $P_{lateral}$ close to zero and the third experiment with positive P_{mean} in subspaces 3 and 4. In subspace 1, the air pressure stayed close to 0 Pa during all experiments. In subspace 2, a drift in the pressure signal has been observed, that was probably caused by ambient pressure changes. No effect of this signal on the CO_2 profiles has been observed. Due to this unstable sensor signal, $P_{lateral}$ was calculated using P_{mean} in subspaces 1 and 3 rather than using P_{mean} in subspace 2. For the different levels of pressure pumping intensity, no detectable reaction of the CO_2 profiles was observed. In the experiment without $P_{lateral}$, where P_{mean} stayed close to 0 Pa in all subspaces,

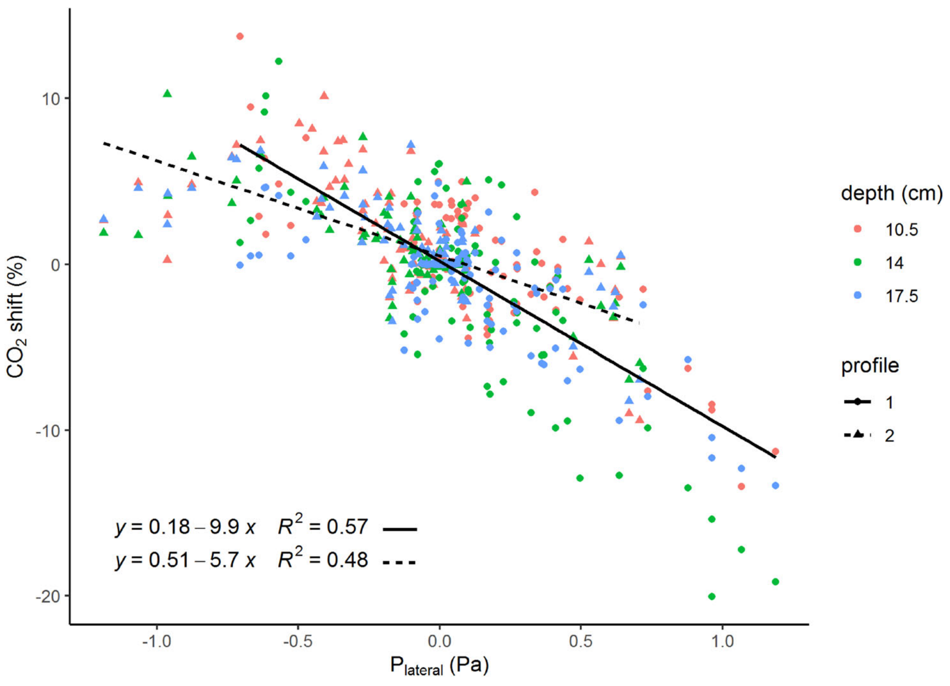

FIGURE 7 Relationship between $P_{lateral}$ and CO_2-*shift*. Data from all experiments are combined. The data are illustrated from depths 3 to 5 of both profiles. The shown regression line is fitted for depths 3 to 5 together.

no clear pattern in CO_2-*shift* was observed. In the other experiments, CO_2-*shift* showed an apparent response to $P_{lateral}$, with reverse patterns in CO_2-*shift* when $P_{lateral}$ was inverted. Interestingly, the pressure in subspace 3 showed a substantial effect on profile 1, which was in the adjacent subspace, indicating that the lateral pressure gradient is creating a flow field in the surrounding soil.

Figure 5 shows the relationship between CO_2-*shift* and *PPC*. For the experiments, where *PPC* was combined with $P_{lateral}$ the effect of $P_{lateral}$ dominates the gas transport and no discernible effect of PPC was observed. When only experiments with $P_{lateral}$ in a range between −0.1 and 0.1 Pa are considered, a slight increase in CO_2-*shift* with higher *PPC* can be observed. However, this relationship is inconsistent over the profiles and the different depths and is probably an artefact, which is discussed in Section 4.2.

3.2 | Static pressure fields

Our experiments observed a strong reaction of the CO_2 profiles on static pressure fields. Figure 6 shows three exemplary experiments with static pressure fields. Both profiles show an increase in CO_2 when relative pressure decreases and a decrease in CO_2 when relative pressure increases. This can be explained by vertical advection caused by the pressure gradients transporting soil gas with higher CO_2 concentrations upwards or air from the atmosphere into the soil. In profile 1, CO_2 concentrations show a strong reaction on $P_{lateral}$. This profile was located closer to the border between the subspaces than profile 2, which shows a less pronounced reaction on $P_{lateral}$. CO_2-*shift* in profile 2 correlates well with P_{mean} in the respective subspace.

An apparent relationship between $P_{lateral}$ and CO_2-*shift* was observed. Figure 7 shows a scatter plot combining data from all 29 experiments. Individual regressions were fit for each depth to compare the reaction of the different depths. The slopes of the individual regressions were steeper in the upper depths and flattened with depth. The weakest reaction was observed in depth 7 (24.5 cm). The effect was consistent from depths 3 to 5 (10.5, 14.0 and 17.5 cm) with a comparable slope (profile 1: −8.5, −13.7 and −7.7; profile 2: −6.4, −5.3 and −5.4, at depths 3, 4 and 5 respectively) and R^2 around 0.5 to 0.6 (p-values <1e-10), only depth 4 of profile 1 stands out with a steeper slope. Therefore, these depths were selected to illustrate the effect. The replications of the experiment and the different depths show consistent behaviour. Pressure gradients between −1 and 1 Pa resulted in a CO_2-*shift* of 8% on average and up to 20% in some cases. The effect is similar among both profiles. CO_2-*shift* in profile 1 shows a stronger reaction on $P_{lateral}$ between the subspaces, whereas CO_2-*shift* in profile 2 can be adequately explained by the pressure in the respective subspace. The location of the profiles inside the chamber can probably explain this. Profile 1 is closer to the border between subspaces 2 and 3. Therefore, the boundary effects from $P_{lateral}$ between these subspaces affect profile 2 stronger. The experiments with and without additional pressure pumping show comparable results indicating that *PPC* has a negligible effect compared to static pressure fields.

4 | DISCUSSION

4.1 | Pressure pumping

No discernible response of the CO_2 profiles on the simulated pressure pumping was observed. We conclude that the effect of pressure pumping on gas transport is negligible in contrast to the advection caused by the observed static lateral pressure gradients, that was dominating during our experiments. When only data without $P_{lateral}$ and with P_{mean} around 0 Pa were considered, a slight increase in *CO_2-shift* with *PPC* could be observed. However, this relationship is inconsistent over the profiles and the different depths, and we believe that this relationship is likely to be an artefact. Based on the process understanding described in the literature, we expect a decrease in CO_2 concentration as a reaction to pressure pumping (Laemmel, Mohr, Schack-Kirchner, et al., 2019; Maier et al., 2012). An increase in CO_2 cannot be explained by increased dispersion when no net mass flow occurs.

The measurements are potentially influenced by small changes in $P_{lateral}$ that have not been detected since the effect of $P_{lateral}$ on *CO_2-shift* was relevant in a range close to the calibration accuracy of the pressure sensors. Additionally, *CO_2-shift* is calculated using interpolated data which raises uncertainty of the results since the CO_2 profiles underlie temporal changes due to changes in soil temperature and other environmental factors affecting soil CO_2 production.

Even though no effect of *PPC* was observed, this does not necessarily mean that the pressure pumping effect does not exist. It remains to be seen whether the artificial pressure pumping is comparable to naturally occurring pressure pumping since it is spatially limited to a small area and the soil column is open to exchange with the surrounding unaffected soil. This decreases the depth to which the pressure oscillations affect gas transport, as documented by Takle et al. (2004), who have conducted similar experiments with artificial pressure pumping. They generated pressure fluctuations by manual pumping on the bottom of a water tank placed upside down on the soil and observed that artificial pressure pumping showed strong attenuation with depth while natural pressure pumping was unattenuated for the first 0.6 m.

4.2 | Static pressure fields

The results show an apparent response of CO_2 profiles on static pressure fields between -1 and 1 Pa. The strength of the effect differed between the two profiles. The different positions of the profiles inside the flow field can explain this. Based on theoretical consideration according to Figure 2, local advective fluxes are expected to be strongest close to the borders between the subspaces where pressure gradients are strongest. The stronger effect of $P_{lateral}$ at profile 1 can be attributed to the location closer to the subspace border. After analysing the results, we found that the time it takes for the concentration profiles to stabilize after each experiment is longer than expected and thus some of the results might have been influenced by the previous experiment. To prevent this, we would recommend lag times of at least 12 h after each experiment when conducting similar experiments in the future.

The results were consistent over several experiments and in line with the process conception illustrated in Figure 2. We assume that the changes in the gas profile are not affected by changes in CO_2 production since respiration in a well-aerated soil is generally not limited by oxygen availability. Hence, the observed changes in concentration profiles are exclusively attributed to changes in gas transport. Since positive and negative pressure gradients led to a reverse response of *CO_2-shift*, we conclude that $P_{lateral}$ causes vertical and lateral advection that can be directed upward or downward depending on the position in the pressure field and the resulting field of airflow in the soil pores. Since the CO_2 production is not affected by the changed concentrations, the enhanced ventilation only causes a storage change in soil air and does not affect the overall CO_2 efflux when integrating over longer time periods (Subke et al., 2003) in an area that covers the high and low-pressurized sections. However, for gases like CH_4, where consumption rates are probably transport-limited (Glagolev et al., 2022; Maier et al., 2017), increased ventilation of soil air could also increase the net CH_4 sink of soil.

Although in this study, lateral pressure gradients were artificially generated, pressure fields in a similar magnitude can be caused, for example, by stable wind flowing around an obstacle which creates lateral pressure gradients between windward and leeward side (Massman, 2006). Takle (2003) states these pressure gradients can range up to 10–20 Pa/m across a windbreak. Amos et al. (2009) observed pressure gradients between -1 and 1 Pa/m caused by wind flowing over a waste rock pile, which is comparable in magnitude to the presented experiments. Similar results can be found in other studies (Brandle, 1995; Funke et al., 2021; Nieveen et al., 2001). The magnitude of the effect probably depends on soil physical parameters like porosity, pore size distribution or tortuosity since they are important factors for gas transport in soil. We expect the effect to be stronger in porous soils with macropores since the pressure-driven advection can propagate deeper and faster into these soils. Especially under wet conditions, when smaller pores are water-saturated macropores play a major role in gas transport and hence also are an important factor for the described effect. Also, soil respiration has an influence on the magnitude of this effect since at a given transport rate, it controls the concentration gradient that arises in soil under steady-state conditions. With a steeper concentration gradient, the same advective flux causes a stronger absolute concentration change. However, in our experiments, we could eliminate the influence of different respiration rates by using *CO_2-shift* which describes the relative concentration change. The effect of static pressure fields on *CO_2-shift* showed comparable results for various experiments with varying respiration rates and resulting concentration gradients in this study.

Other studies have shown wind speed effects on soil gas transport (Adisaputro et al., 2021; Reicosky et al., 2008; Takle et al., 2004) or gas transport in snow (Bowling & Massman, 2011; Fujiyoshi et al., 2010). However, in most of these studies, the forcing pressure gradients have not been measured directly, and it cannot be differentiated between the effect of static pressure fields generated by the wind, mixing of the surface air, ventilating the ground vegetation or litter layer and wind-induced pressure pumping, since all these phenomena correlate with wind speed. With the described chamber system, we can exclude the influence of wind speed directly above the soil and separate the effect of static pressure fields and pressure pumping from other influences.

Takle et al. (2004) investigated pressure effects generated by a fence that created static and oscillating pressure fields. They concluded that in their set-up, local pressure fields generated by the fence affected gas transport and non-local pressure fluctuations were magnitudes smaller than locally generated fluctuations. They focused on locally generated pressure fluctuations rather than static pressure gradients as they have higher amplitudes. In contrast to that, our results suggest that static pressure fields dominate the effect even if they are in a smaller magnitude than peak-to-valley variations of pressure fluctuations.

Additionally, the results of this study point out the susceptibility of chamber measurements to artefacts caused by pressure gradients. Pressure gradients between chamber systems and the atmosphere are known to be problematic. Longdoz et al. (2000) experimented with flow rates in a steady-state flow-through chamber. They showed that marginal pressure gradients between the chamber and ambient pressure caused by the divergence of inflow and outflow rates substantially affects the resulting flux estimates. Lund et al. (1999) showed that pressurization by dynamic chamber systems results in advection that disrupts the concentration gradient at the soil-atmosphere interface, which directly affects diffusion rates. In closed dynamic chambers, pressure gradients can be caused by the Venturi effect under windy conditions if the vent design is inappropriate (Xu et al., 2006). This is a well-known effect which is considered in most chamber designs. Xu et al. (2006) observed pressure deviations between −15 and 8 Pa in chambers with no appropriate vent design under windy conditions, which causes strongly biased flux estimates. But even the mere presence of the chamber might create lateral pressure gradients by the airflow around the chamber under windy conditions. Even if this wind-induced pressure field only affects pressure outside the chamber and pressure inside the chamber is equal to the average ambient pressure, this could yield biased results since we observed that pressure fields also influence gas transport in the surrounding soil. Also, excluding wind inside the chamber is a disturbance that must be considered. Zawilski (2022) presented a method to correct for the influence of wind speed on evaporation rates in chamber measurements by varying the fan speed inside a chamber system.

Fans operating inside chambers used for head-space mixing can cause local pressure fields inside the chamber when fan speed is high. Especially in large chamber systems (e.g., used for maize), strong fans are needed. In preliminary tests, we observed pressure gradients inside the individual subspaces caused by fans installed directly above the soil when we experimented with different fan speeds (data shown in Appendix S1, S2). These pressure fields had a comparable effect on the gas profiles as the presented pressure fields between the subspaces. However, these effects were not analysed systematically in this study. Therefore, the effect of wind generated by the fans inside the chamber is probably not comparable to the wind conditions in the absence of the chamber. This should be considered when using fans for head-space mixing in flux chambers. Especially in big chambers, it might be better to use several small fans rather than one big fan.

A flux estimation based on the observed CO_2 profiles was not conducted since the gradient method approach assumes pure diffusive fluxes (Maier & Schack-Kirchner, 2014), and advective fluxes disrupt the CO_2 profile that arises under purely diffusive conditions. A rise in CO_2 would mean a decrease in flux when assuming diffusion only and production stays constant. When considering bulk flow, rising concentrations can also result from the vertical transport of gas from depths with higher CO_2 concentrations. Therefore, when non-diffusive transport occurs, more complex numerical flux estimation models must be used, like the model presented by Massman and Frank (2022).

5 | CONCLUSIONS

The presented chamber system could simulate pressure fields in a realistic range. No effect of the simulated pressure pumping on the CO_2 profiles was observed. However, it remains to be seen whether the simulated pressure pumping can be directly compared to natural pressure pumping since it affects a much smaller area and boundary effects with the surrounding unaffected soil cannot be excluded.

This study observed an apparent effect of static pressure fields on gas concentration profiles. These concentration changes were probably caused by advective gas fluxes generated by lateral pressure gradients. Results show that the position of the observed profile relative to the forcing pressure gradient is important and point measurements do not represent the entire flow field. Even very small pressure gradients around 1 Pa resulted in a *CO_2-shift* of 8% on average. To identify the dependency of this phenomenon on soil physical parameters, further investigations in different soil types are needed.

On the one hand, the presented results indicate that naturally occurring static pressure fields resulting from wind interacting with topographic features can enhance gas exchange between soil and atmosphere. On the other hand, the results indicate that, when conducting chamber flux measurements, pressure gradients inside the chamber and the surrounding soil must be avoided since they can result in advective fluxes which would strongly bias the results. Additionally, chamber measurements under windy conditions are potentially biased due to wind-induced pressure fields that might be affected by the mere presence of the chamber.

AUTHOR CONTRIBUTIONS

Laurin Osterholt: Conceptualization; methodology; software; visualization; writing – original draft; data curation; investigation; formal analysis; validation. **Martin Maier:** Writing – review and editing; supervision; conceptualization; project administration; funding acquisition; methodology; investigation; formal analysis; validation; resources. **Dirk Schindler:** Writing – review and editing; funding acquisition; resources.

ACKNOWLEDGEMENTS

We thank Alfred Baer for the technical support and his ideas in the development of the chamber system. We also thank our colleagues from the Chair of Environmental Meteorology at the University of Freiburg for the support and access to their experimental site. This research was supported by the German Research Foundation (DFG, MA 5826/2-2). Open Access funding enabled and organized by Projekt DEAL.

DATA AVAILABILITY STATEMENT

The data that support the findings of this study are available from the corresponding author upon reasonable request.

ORCID

Martin Maier https://orcid.org/0000-0002-7959-0108

REFERENCES

Adisaputro, D., De Donato, P., Saint-Andre, L., Barres, O., Galy, C., Nourrisson, G., Piedevache, M., & Derrien, M. (2021). Baseline subsoil CO_2 gas measurements and micrometeorological monitoring: Above canopy turbulence effects on the subsoil CO_2 dynamics in temperate deciduous Forest. *Applied Sciences*, *11*, 1753.

Amos, R. T., Blowes, D. W., Smith, L., & Sego, D. C. (2009). Measurement of wind-induced pressure gradients in a waste rock pile. *Vadose Zone Journal*, *8*, 953–962.

Bahlmann, L. M., Smits, K. M., Heck, K., Coltman, E., Helmig, R., & Neuweiler, I. (2020). Gas component transport across the soil-atmosphere interface for gases of different density: Experiments and modeling. *Water Resources Research*, *56*, e2020WR027600.

Bowling, D. R., & Massman, W. J. (2011). Persistent wind-induced enhancement of diffusive CO_2 transport in a mountain forest snowpack. *Journal of Geophysical Research*, *116*, G04006.

Brandle, J. R. (1995). Static pressure at the ground under atmospheric flow across a windbreak.

Clarke, G. K. C., & Waddington, E. D. (1991). A three-dimensional theory of wind pumping. *Journal of Glaciology*, *37*, 89–96.

Clements, W. E., & Wilkening, M. H. (1974). Atmospheric pressure effects on ^{222}Rn transport across the earth-air interface. *Journal of Geophysical Research*, *79*, 5025–5029.

Elberling, B. (2003). Seasonal trends of soil CO_2 dynamics in a soil subject to freezing. *Journal of Hydrology*, *276*, 159–175.

FAO. (2006). *World reference base for soil resources, 2006: A framework for international classification, correlation, and communication* (2006th ed.). Food and Agriculture Organization of the United Nations.

Fujiyoshi, R., Haraki, Y., Sumiyoshi, T., Amano, H., Kobal, I., & Vaupotič, J. (2010). Tracing the sources of gaseous components (222 Rn, CO 2 and its carbon isotopes) in soil air under a cool-deciduous stand in Sapporo, Japan. *Environmental Geochemistry and Health*, *32*, 73–82.

Funke, C. S., Buckley, M. P., Schultze, L. K. P., Veron, F., Timmermans, M.-L. E., & Carpenter, J. R. (2021). Pressure fields in the airflow over wind-generated surface waves. *Journal of Physical Oceanography*, 3449–3460. Accessed: 6/2/2023. https://journals.ametsoc.org/view/journals/phoc/aop/JPO-D-20-0311.1/JPO-D-20-0311.1.xml

Glagolev, M. V., Glagolev, M. V., Suvorov, G. G., Suvorov, G. G., Il'yasov, D. V., Il'yasov, D. V., Sabrekov, A. F., Sabrekov, A. F., Terentieva, I. E., & Terentieva, I. E. (2022). What is the maximal possible soil methane uptake? *Environmental Dynamics and Global Climate Change*, *13*, 123–141.

Laemmel, T., Mohr, M., Longdoz, B., Schack-Kirchner, H., Lang, F., Schindler, D., & Maier, M. (2019). From above the forest into the soil – How wind affects soil gas transport through air pressure fluctuations. *Agricultural and Forest Meteorology*, *265*, 424–434.

Laemmel, T., Mohr, M., Schack-Kirchner, H., Schindler, D., & Maier, M. (2019). 1D air pressure fluctuations cannot fully explain the natural pressure-pumping effect on soil gas transport. *Soil Science Society of America Journal*, *83*, 1044–1053.

Levintal, E., Dragila, M. I., Zafrir, H., & Weisbrod, N. (2020). The role of atmospheric conditions in CO_2 and radon emissions from an abandoned water well. *Science of the Total Environment*, *722*(137), 857.

Longdoz, B., Yernaux, M., & Aubinet, M. (2000). Soil CO $_2$ efflux measurements in a mixed forest: Impact of chamber disturbances, spatial variability and seasonal evolution: SOIL CO $_2$ EFFLUX IN a MIXED FOREST. *Global Change Biology*, *6*, 907–917.

Lund, C. P., Riley, W. J., Pierce, L. L., & Field, C. B. (1999). The effects of chamber pressurization on soil-surface CO2 flux and the implications for NEE measurements under elevated CO2. *Global Change Biology*, *5*, 269–281.

Maier, M., Paulus, S., Nicolai, C., Stutz, K., & Nauer, P. (2017). Drivers of plot-scale variability of CH_4 consumption in a well-aerated pine Forest soil. *Forests*, *8*, 193.

Maier, M., & Schack-Kirchner, H. (2014). Using the gradient method to determine soil gas flux: A review. *Agricultural and Forest Meteorology*, *192–193*, 78–95.

Maier, M., Schack-Kirchner, H., Aubinet, M., Goffin, S., Longdoz, B., & Parent, F. (2012). Turbulence effect on gas transport in three contrasting Forest soils. *Soil Science Society of America Journal*, *76*, 1518–1528.

Maier, M., Schack-Kirchner, H., Hildebrand, E. E., & Schindler, D. (2011). Soil CO_2 efflux vs. soil respiration: Implications for flux models. *Agricultural and Forest Meteorology*, *151*, 1723–1730.

Maier, M., Weber, T. K., Fiedler, J., Fuss, R., Glatzel, S., Huth, V., Jordan, S., Jurasinski, G., Kutzbach, L., & Schäfer, K. (2022). Introduction of a guideline for measurements of greenhouse gas fluxes from soils using non-steady-state chambers. *Journal of Plant Nutrition and Soil Science*, *185*, 447–461.

Massman, W. J. (2006). Advective transport of CO $_2$ in permeable media induced by atmospheric pressure fluctuations: 1. An analytical model. *Journal of Geophysical Research*, *111*, G03004.

Massman, W. J., & Frank, J. M. (2022). Modeling gas flow velocities in soils induced by variations in surface pressure, heat and moisture dynamics. *Journal of Advances in Modeling Earth Systems*, *14*, e2022MS003086. Accessed: 26/9/2022. https://onlinelibrary.wiley.com/doi/10.1029/2022MS003086

Mohr, M., Laemmel, T., Maier, M., & Schindler, D. (2016). Analysis of air pressure fluctuations and topsoil gas concentrations within a scots pine Forest. *Atmosphere*, *7*, 125.

Mohr, M., Laemmel, T., Maier, M., & Schindler, D. (2020). Inexpensive high-precision system for measuring air pressure fluctuations. *Meteorological Applications*, *27*, e1815. Accessed: 15/9/2020. https://onlinelibrary.wiley.com/doi/abs/10.1002/met.1815

Nieveen, J. P., El-Kilani, R. M. M., & Jacobs, A. F. G. (2001). Behaviour of the static pressure around a tussock grassland–forest interface. *Agricultural and Forest Meteorology*, *106*, 253–259.

Osterholt, L., Kolbe, S., & Maier, M. (2022). A differential CO $_2$ profile probe approach for field measurements of soil gas transport and soil respiration [#]. *Journal of Plant Nutrition and Soil Science*, *185*, 282–296.

R Core Team. (2021). *A language and environment for statistical computing*. R Foundation for Statistical Computing. https://www.R-project.org

Rajewski, D. A., Takle, E. S., Lundquist, J. K., Prueger, J. H., Pfeiffer, R. L., Hatfield, J. L., Spoth, K. K., & Doorenbos, R. K. (2014). Changes in fluxes of heat, H_2O, and CO_2 caused by a large wind farm. *Agricultural and Forest Meteorology*, *194*, 175–187.

Reicosky, D. C., Gesch, R. W., Wagner, S. W., Gilbert, R. A., Wente, C. D., & Morris, D. R. (2008). Tillage and wind effects on soil CO_2 concentrations in muck soils. *Soil and Tillage Research*, *99*, 221–231.

Scanlon, B. R., Nicot, J. P., & Massmann, J. W. (2002). Soil gas movement in unsaturated systems. *Soil Physics Companion*, *389*, 297–341.

Schlesinger, W. H., & Andrews, J. A. (2000). Soil respiration and the global carbon cycle. *Biogeochemistry*, *48*, 7–20.

Smith, K. A., Ball, T., Conen, F., Dobbie, K. E., Massheder, J., & Rey, A. (2003). Exchange of greenhouse gases between soil and atmosphere: Interactions of soil physical factors and biological processes. *European Journal of Soil Science*, *54*, 779–791.

Subke, J.-A., Reichstein, M., & Tenhunen, J. D. (2003). Explaining temporal variation in soil CO_2 efflux in a mature spruce forest in southern Germany. *Soil Biology and Biochemistry*, *35*, 1467–1483.

Takle, E. (2003). High-frequency pressure variations in the vicinity of a surface CO_2 flux chamber. *Agricultural and Forest Meteorology*, *114*, 245–250.

Takle, E. S., Massman, W. J., Brandle, J. R., Schmidt, R. A., Zhou, X., Litvina, I. V., Garcia, R., Doyle, G., & Rice, C. W. (2004). Influence of high-frequency ambient pressure pumping on carbon dioxide efflux from soil. *Agricultural and Forest Meteorology*, *124*, 193–206.

Wood, S. N. (2017). *Generalized additive models: An introduction with R*. CRC press.

Xu, L., Furtaw, M. D., Madsen, R. A., Garcia, R. L., Anderson, D. J., & McDermitt, D. K. (2006). On maintaining pressure equilibrium between a soil CO_2 flux chamber and the ambient air. *Journal of Geophysical Research*, *111*, D08S10.

Zawilski, B. M. (2022). Wind speed influences corrected autocalibrated soil Evapo-respiration chamber (ASERC) evaporation measures. *Geoscientific Instrumentation, Methods and Data Systems*, *11*, 163–182.

SUPPORTING INFORMATION

Additional supporting information can be found online in the Supporting Information section at the end of this article.

How to cite this article: Osterholt, L., Maier, M., & Schindler, D. (2023). Small lateral air pressure gradients generated by a large chamber system have a strong effect on CO_2 transport in soil. *European Journal of Soil Science*, *74*(4), e13405. https://doi.org/10.1111/ejss.13405